ResearchGate

See discussions, stats, and author profiles for this publication at: https://www.researchgate.net/publication/21366260

# Structural properties of polydisperse biopolymer solutions: A light scattering study of bovine ?-crystallin

**ARTICLE** *in* BIOPOLYMERS · SEPTEMBER 1991

Impact Factor: 2.39 · DOI: 10.1002/bip.360311011 · Source: PubMed

CITATIONS
51

READS
9

**2 AUTHORS:**

Peter Schurtenberger
Lund University
**263** PUBLICATIONS **7,682** CITATIONS
SEE PROFILE

Robert Augusteyn
Brien Holden Vision Institute
**141** PUBLICATIONS **3,283** CITATIONS
SEE PROFILE

Available from: Robert Augusteyn
Retrieved on: 22 January 2016

# Structural Properties of Polydisperse Biopolymer Solutions: A Light Scattering Study of Bovine $\alpha$-Crystallin

P. SCHURTENBERGER[1,*] and R. C. AUGUSTEYN[2]

[1] Department of Physics and Center for Materials Science and Engineering, Massachusetts Institute of Technology, Cambridge Massachusetts 02139; [2] Biochemistry Department, Melbourne University, Victoria 3052, Australia

**SYNOPSIS**

We have measured $\langle R_H \rangle_z$, $\langle R_G^2 \rangle_z^{1/2}$, and $\langle M \rangle_w$ for individual fractions of the protein $\alpha$-crystallin obtained by gel filtration of bovine lens nuclear extracts. A strong and monotonic decrease of $\langle R_H \rangle_z$ and $\langle M \rangle_w$ with increasing elution volume could be observed, indicating a broad size distribution. The experimental results are quantitatively consistent with a polymerization of monomeric units into linear chains, which may have a certain degree of flexibility. Using theoretical expressions for $\langle R_G^2 \rangle$ and $R_H$ originally derived for semiflexible polymers in solution, we can self-consistently analyse the data from static and dynamic light scattering, and from electron microscopy experiments. We thus obtain detailed information on the molecular weight distribution and the quaternary structure of $\alpha$-crystallin in these solutions.

## INTRODUCTION

$\alpha$-Crystallin, the major mammalian lens protein, is a large multisubunit protein. The protein can be easily obtained in large quantities, and an enormous range of chemical, hydrodynamic, and immunological studies on $\alpha$-crystallin can be found in the literature. Its function appears to be only structural, i.e., as a part of the "space-filling material" of the eye lens. Despite the large amount of experimental data collected in the past and the protein's simple function, the current understanding of the protein is still vague and imprecise. Even the answer to the apparently simple question of the molecular weight of $\alpha$-crystallin remains a matter of considerable controversy in the literature. Attempts to determine the quaternary structure of $\alpha$-crystallin have been hampered by the polydispersity of the protein as normally isolated. The most commonly studied form of the protein consists of species with molecular weights of 800,000 ± 200,000,[1,2] but species ranging from a low of 280,000 (see Ref. 10) to a high of >10,000,000 (see Ref. 3) have also been isolated. This polydispersity appears to arise from posttranslational modification[4] and from formation of chain-like structures,[5,6] which both increase with increasing age of the lens. Relatively few investigators have attempted to reduce this heterogeneity prior to structural studies or even to allow for it in their interpretations.

The polydispersity of $\alpha$-crystallin preparations can be significantly reduced by isolating the protein from fetal tissues and by careful fractionation.[7] This yields the minimum species population, which represents about 30% of the total and has a molecular weight around 500,000 if isolated at 4°C and around 280,000 when isolated at 37°C. The protein can also be reassembled after complete disruption with chaotropic agents. The molecular weights of the ensembles produced at low ionic strengths[6,8,9] are in the range of 200,000–300,000, while at high ionic strengths[10] molecular weights of around 500,000 are produced. These observations suggest that the protein can exist in several different low molecular weight forms. The relationship between the various molecular weight forms of the protein is not yet understood.

Electron microscopy has suggested that the various $\alpha$-crystallins may be formed by polymerization

Biopolymers, Vol. 31, 1229–1240 (1991)
© 1991 John Wiley & Sons, Inc.
CCC 0006-3525/91/101229-12$04.00

* Present address: Institut für Polymere, ETH Zürich, 8092 Zürich, Switzerland

of a smaller monomer unit. Siezen et al.[6] found that high molecular weight $\alpha$-crystallins were composed of chain-like polymers of spherical particles with diameters of 120–140 Å. Similar observations have been made in our laboratories with both reconstituted $\alpha$-crystallins and restricted populations isolated by gel filtration.[5,11] However, as attractive a technique as electron microscopy appears to be for direct structural investigations of large protein aggregates, its successful application requires that the sample preparation procedure does not alter the conformation and size distribution of the protein complexes. This introduces a constant source of errors and artefacts. In addition to the uncertainty coming from the sample preparation procedures required, errors can arise from operator bias in selection of too few small (or large) complexes and the fact that three-dimensional quantities are estimated from an image in two dimensions on the photomicrograph.

Enormous progress has been made theoretically as well as experimentally on the characterization and understanding of polymer conformation in solution. In particular, the application of static (SLS) and dynamic light scattering (QLS) to polymer solutions and the development of theories that permit a calculation of the radius of gyration $R_G$, the particle scattering factor $P(Q)$, and the translational and rotational diffusion coefficients $D_t$ and $D_r$, respectively, of polymers in solution as a function of their molecular weight and conformation, has been very successful.[12–15] However, while these recent developments have been beneficial for polymer science, they have remained quite unnoticed by the majority of biochemists and biophysicists. As a consequence, these modern trends in polymer physics have had only a minor impact on studies of biopolymers.

In protein research, scattering techniques are primarily used to routinely determine the average molecular weight of individual proteins or their tertiary structure (conformation) in a crystal lattice. As in the case of synthetic polymers, however, light scattering permits, in principle, a fast and noninvasive study of the size and shape of biopolymers in solution. Particularly, the dynamic light scattering technique profits from the enormous experimental and theoretical progress made during the past few years.[16,17] However, if used for a characterization of polydisperse solutions, light scattering can, in general, only provide average quantities such as a $z$-average hydrodynamic radius $\langle R_H \rangle_z$ or a $z$-average mean square radius of gyration $\langle R_G^2 \rangle_z$. Also, one always has to keep in mind that light scattering, like x-ray or neutron scattering, is an indirect technique for determining size, shape, and structure of macromolecules, and only allows for a self-consistent data analysis and interpretation based on explicit structural models and assumptions for the intra- and intermolecular interaction effects.

It is the aim of this article to show that additional and detailed information on the structure and size distribution of biopolymers such as proteins can be obtained by making analogies to polymer solutions and using modern polymer theory for an interpretation of data from scattering experiments. Special emphasis will be made on a combination of gel filtration, electron microscopy, and light scattering, which provides independent and complimentary information, and offers a direct test of the respective results from the different techniques. This experimental approach has been used successfully for the characterization of polydisperse solutions of vesicles, and for a study of the size and structure of antigen–antibody complexes.[18–20]

## STATIC AND DYNAMIC LIGHT SCATTERING FROM MACROMOLECULES IN SOLUTION: THEORETICAL BACKGROUND

In a static light scattering experiment (SLS), the intensity of the scattered light is measured at a scattering vector $Q$, where $|Q| = (4\pi n/\lambda_0)\sin(\theta/2)$, $\theta$ is the scattering angle, $n$ is the refractive index of the solution, and $\lambda_0$ is the wavelength of the incident light in vacuo. For a quantitative analysis of the SLS experiments, a reduced intensity, the so-called excess Rayleigh ratio, $\Delta\mathbf{R}(\theta)$ (i.e., the differential cross section of the scattering process) is generally used. For dilute macromolecular solutions, $\Delta\mathbf{R}(\theta)$ can be represented by[21]

$$\frac{K \cdot C}{\Delta\mathbf{R}_s(\theta)} = \frac{1}{P(\theta)}\left(\frac{1}{\langle M \rangle_w} + 2BC + \cdots\right) \quad (1)$$

where $K = 4\pi^2 n^2 (dn/dc)^2 / N_A \cdot \lambda_0^4$, $dn/dc$ is the refractive index increment, $C$ is the concentration in milligrams per milliliter, $P(\theta)$ is the particle form factor, $\langle M \rangle_w$ is the weight average molecular weight of the particles in solution, and $B$ is the second virial coefficient. The particle form factor describes the influence of intraparticle interference effects on the angular dependence of the scattered intensity, and thus provides information on the macromolecular

shape and structure. In the limit of small values of $Q \cdot R_G$, one can use the following expansion of $P(\theta)$[21]

$$P(\theta) = 1 - \frac{Q^2 \cdot R_G^2}{3} + \cdots \quad (2)$$

and Eq. (1) can be simplified in the limit of low concentrations to

$$\frac{K \cdot C}{\Delta \mathbf{R}_s(\theta)} = \frac{1}{\langle M \rangle_w} (1 + \tfrac{1}{3} \cdot Q^2 \langle R_G^2 \rangle_z) \quad (3)$$

where $\langle R_G^2 \rangle_z$ is the $z$-average mean square radius of gyration. It is therefore possible to determine from the $Q$ dependence of the scattered intensity $\Delta \mathbf{R}_s(\theta)$, in the limit of small $Q$, the radius of gyration independently of the shape of the particle. This ability to obtain an experimental value for the radius of gyration provides a powerful tool in the determination of macromolecular structure, since macromolecules of different configurational types (e.g., solid spheres, rods, flexible chains, random coils) have quite different values of the radius of gyration for the same value of the molecular weight.

In a dynamic or quasielastic light scattering experiment (QLS), the intensity autocorrelation function $G_2(\vec{Q}, \tau) = \langle I(\vec{Q}, 0) I(\vec{Q}, \tau) \rangle$ is measured, where $I(\vec{Q}, 0)$ and $I(\vec{Q}, \tau)$ are the scattering intensities at time $t = 0$ and $t = \tau$, respectively. From $G_2$ one can extract the dynamic structure factor $S(\vec{Q}, \tau)$, which describes the dynamics of intra- and intermolecular motion.[22] For dilute and monodisperse solutions of small macromolecules, $G_2$ decays like a single exponential. However, $G_2$ cannot be described by a single exponential for polydisperse solutions and large flexible macromolecules with dimensions exceeding $\lambda/20$. Under these conditions, a cumulant expansion of $G_2$ is generally used to analyze QLS experiments,[23]

$$\ln |g_1(\tau)| = -\langle \Gamma \rangle \cdot \tau + \tfrac{1}{2} \cdot \mu_2 \cdot (\Gamma \tau)^2 \quad (4)$$

where $g_1(\tau)$ is the normalized field autocorrelation function {with $g_1(\tau) = [(G_2(\tau) - B)/B]^{1/2}$, and $B$ is the experimentally determined baseline of the intensity autocorrelation function}, $\langle \Gamma \rangle$ is the first cumulant, and $\mu_2$ is a dimensionless quantity that depends on polydispersity and internal flexibility of the macromolecule. The first cumulant can then be expressed by[15]

$$\langle \Gamma \rangle / Q^2 = \langle D \rangle_z \cdot (1 + C \cdot Q^2 \cdot \langle R_G^2 \rangle_z + \cdots) \quad (5)$$

where $\langle D \rangle_z$ is the $z$-average translational diffusion coefficient, and $C$ a dimensionless quantity that depends on the structure, flexibility, and polydispersity of the macromolecules. The reciprocal of the $z$-average inverse hydrodynamic radius, denoted by $\langle R_H \rangle_z$, can then be calculated from $\langle D \rangle_z$ by using the Stokes–Einstein relation,

$$\langle R_H \rangle_z := \left\langle \frac{1}{R_H} \right\rangle_z^{-1} = \frac{k_B T}{6 \pi \eta \langle D \rangle_z} \quad (6)$$

where $\eta$ is the viscosity of the solvent. The hydrodynamic radius contains information on both the structure and the polydispersity. A combination of static and dynamic light scattering, i.e., simultaneous measurements of the quantities $\langle M \rangle_w$, $\langle R_G^2 \rangle_z$, and $\langle R_H \rangle_z$ thus permits a precise and detailed characterization of the structure and size distribution of macromolecules in solution.

This experimental approach is particularly helpful when combined with an analysis of the results based on theoretical expressions for the radius of gyration and the hydrodynamic radius for different structural models. A number of polymer systems show conformational behavior intermediate to that of rigid rods and random coils. A frequently employed model for semiflexible macromolecules is the Kratky–Porod wormlike chain.[13] This model describes semiflexible chains in terms of a persistence length $l_p$, which is a measure of chain stiffness. Reliable theoretical expressions for the radius of gyration and the hydrodynamic radius as a function $l_p$, of chain diameter $d$, and of chain contour length $L$, exist for this model.[13,14] Based on this model, detailed theoretical and experimental investigations on the influence of chain flexibility and polydispersity on SLS and QLS were previously conducted. Similar expressions have been derived for the two limiting cases, i.e., for rigid cylinders and random coils, as well as for other geometries such as oblate or prolate ellipsoids, for example.[24–26]

## MATERIALS AND METHODS

### Sample Preparation

$\alpha$-Crystallins were isolated from extracts of bovine lens nuclei by gel filtration on Sepharose CL4B in 0.05 $M$ Tris HCl, 1 m$M$ EDTA, pH 8.0, at 4°C, as described by Thomson and Augusteyn.[2] Individual fractions from the Sepharose CL4B column were examined by dynamic light scattering within 3 h of

collection and by static light scattering within 2 days. It was shown that there was no change in the properties of the proteins during the storage at 4°C. Most measurements were made with protein concentrations of 0.5–1.0 mg/mL, in the above buffer, as determined from the absorbance at 280 nm.[8]

## Electron Microscopy

Electron microscopy was performed using a Philips 420 transmission electron microscope fitted with a liquid nitrogen antidecontamination device. Samples of the proteins, at 0.5 mg/mL, were loaded onto Formvar and carbon-coated electron microscope grids and were negatively stained for 20 s with unbuffered 2% aqueous uranyl acetate. Photographs were taken at a magnification of 172,000 as determined by calibration photographs of myosin rod sheets, which exhibit a spacing of 14.3 nm.[27] Particle dimensions were determined from the original negatives at ×10 magnification using a Mitutoyo optical comparator with a digitized micrometer-driven stage. The precision of these measurements was ±1 μm. Data sets ($n > 1000$) were statistically evaluated for mean, standard deviation, and goodness of fit to a normal distribution. Details are given elsewhere.[5]

## Light Scattering

The static and dynamic light scattering experiments were performed on a light scattering spectrometer resembling the instrument devised by Haller, Destor, and Cannell.[28] An argon ion laser (model 90-5, Coherent, Inc., CA) operating at a wavelength $\lambda_0 = 488$ nm is used as the light source. The scattered light can be detected at 12 fixed angles $\theta$ ($11.5° \leq \theta \leq 162.6°$). Computer-controlled solenoid-actuated shutters are used to select one of the 12 scattering angles or the attenuated transmitted laser beam for the measurement. The collected light is guided from the shutters to a single photomultiplier tube (model 9863A-100, EMI, United Kingdom) by optical fibers (model HC-1006-T, Ensign-Bickford, CT). A dust-free water bath provides temperature control and refractive index matching to the sample glass cell. Measurements were performed at a temperature of 20.0 ± 0.01°C.

Eight milliliters of solution were transferred into a cylindrical glass cell (30 mm inner diameter × 32 mm outer diameter). The cell was sealed and the solution was then filtered continuously through a closed-loop system using a Millex GV 0.22-μm filter (Millipore) until telescopic inspection of the scattered light at a scattering angle of 17.4° showed the sample to be free of dust. Absorbance of the samples at 280 nm was measured after the light scattering experiment to ensure that no change in concentration occurred due to filtration or adsorption.

***Static light scattering.*** The key features of the measurement protocol for static measurements were as follows: (a) rapid and 50 times repeated sequential sampling of the transmitted beam intensity $I_0$ and the scattered light intensity at each angle $I(\theta)$, (b) normalization of $I(\theta)$ with $I_0$, and (c) averaging of $I(\theta)/I_0$ using a dust-discrimination procedure described in Haller et al.[28] The average values of $I(\theta)/I_0$ so obtained will be denoted by $\langle I(\theta)/I_0 \rangle$. This protocol reduces inaccuracies due to drifts in laser power and photomultiplier response, and automatically corrects $I(\theta)$ for sample turbidity for cylindrical scattering cells. The background stray light and solvent contributions $\langle I_b(\theta)/I_0 \rangle$ were then measured using the same cell containing highly purified and filtered water and subtracted from $\langle I(\theta)/I_0 \rangle$. To obtain absolute values of the scattered intensity, the average values $\Delta\langle I(\theta)/I_0 \rangle$ were normalized with respect to the intensity $\langle I_{ref}(\theta)/I_0 \rangle$ from the pure, isotropically scattering reference solvents water (purified using a Milli-Q filtration system) and benzene (Aldrich, spectrophotometric grade). The excess Rayleigh ratio of the sample $\Delta\mathbf{R}_s(\theta)$ was then calculated from

$$\Delta\mathbf{R}_s(\theta) = \frac{\Delta\langle I(\theta)/I_0 \rangle}{\langle I_{ref}(\theta)/I_0 \rangle} \cdot \mathbf{R}_{ref}(\theta) \cdot \left(\frac{n}{n_{ref}}\right)^2 \quad (7)$$

where $\mathbf{R}_{ref}(\theta)$ is the Rayleigh ratio of the reference solvent, and $n$ and $n_{ref}$ are the index of refraction of the solution and the reference solvent, respectively.[29] Values used were $\mathbf{R}_{ref}(\theta) = 2.54 \cdot 10^{-4}$ m$^{-1}$ for water and $\mathbf{R}_{ref}(\theta) = 35.4 \cdot 10^{-4}$ m$^{-1}$ for benzene, respectively.[30] An apparent weight-average molecular weight $\langle M \rangle_w$ and a $z$-average mean-square radius of gyration $\langle \mathbf{R}_G^2 \rangle_z$ of the particles in solution were obtained from a least-squares fit of Eq. (3) to the data for $\Delta\mathbf{R}_s(\theta)$. A value of $(dn/dc) = 0.19 \cdot 10^{-3}$ mL/mg was used.[31]

***Dynamic light scattering.*** Dynamic light scattering measurements were made at five different scattering angles (23°, 36.9°, 60.2°, 90.0°, and 162.6°) using a Langley-Ford (Model 1096, Langley-Ford Instruments, FL) correlator. A $z$-average translational diffusion coefficient $\langle D \rangle_z$ and a polydispersity index

$V$ as defined in Ref. 32 was determined by means of a second-order cumulant analysis of the intensity autocorrelation function.[23] From $\langle D \rangle_z$ an apparent hydrodynamic radius $\langle R_H \rangle_z$ was calculated using the Stokes–Einstein relation [Eq. (6)].

***Performance of the Light Scattering Spectrometer.*** A series of tests has been performed in order to verify the proper functioning of the instrument, and to assess the limits and accuracies of the determination of $\langle R_G^2 \rangle_z^{1/2}$, $\langle R_H \rangle_z$, and $\langle M \rangle_w$:

1. First, the stability, angular resolution, and reproducibility of the measurement of the scattered light intensity was investigated by repeatedly measuring the ratio $\langle I(\theta)/I_0 \rangle$ from highly purified water over a period of 24 h. Within this time, the maximum deviation of $\langle I(\theta)/I_0 \rangle$ from its initial value was found to be 0.3% for the smallest angle used ($\theta = 11.5°$). Averaged over all angles, the deviation between two measurements taken 24 h apart was 0.1%.
2. Stability and reproducibility of the absolute calibration of the spectrometer upon changes of the scattering cell and sample was tested by measuring the intensity of light from a sample of pure toluene repeatedly over a period of 24 h. For each measurement, toluene was pipetted into the scattering cell, which was then inserted into the spectrometer. Averaged over all angles, the deviation between two measurements of $\langle I_{ref}(\theta)/I_0 \rangle$ taken 24 h apart was $\leq$0.2%.
3. The consistency between dynamic and static light scattering measurements was tested by determining $\langle R_G^2 \rangle_z^{1/2}$ and $\langle R_H \rangle_z$ for dilute aqueous solutions of monodisperse polystyrene spheres. For the polystyrene sphere solutions we studied, the relationship $R_H = (5/3)^{1/2} \cdot R_G$ was satisfied to within 1% for spheres with $\langle R_G^2 \rangle_z^{1/2} = 337$ Å and to within 1.5% for spheres with $\langle R_G^2 \rangle_z^{1/2} = 145$ Å.

The high sensitivity and stability of the spectrometer enable us to accurately measure the absolute scattered intensities of light scattered from protein solutions, at very low protein concentrations and at low scattering angles. In particular, the high stability of the measured values of $\langle I(\theta)/I_0 \rangle$ for individual angles extend the range of measurable $\langle R_G^2 \rangle_z^{1/2}$ to a lower limit of 80 Å, which corresponds to a dissymetry of $\simeq$2.5% for $\langle I(\theta)/I_0 \rangle$ over the accessible range of scattering angles.

## RESULTS

The size distribution of $\alpha$-crystallins from the cortex of the lens was found to be quite narrow. Therefore, only the nuclear proteins were examined in detail. As discussed below, these were very heterogeneous, presumably reflecting the effects of accumulated age-related changes. Part of the gel permeation elution profile, corresponding to the $\alpha$-crystallin peak, is reproduced in Figure 1A. It should be emphasized that the proteins were all isolated at 4°C, and hence are in the form named $\alpha_c$-crystallin by Thomson and Augusteyn.[2] This is the form most commonly studied in other laboratories.[1,3,6,9,10,33–35]

Individual fractions from the $\alpha$-crystallin peak were studied using dynamic and static light scattering. Many of the same fractions were also examined by electron microscopy, thus permitting a direct comparison of the results obtained with these techniques. The light scattering results obtained with two independent sets of protein samples are summarized in Figure 1B–D.

The hydrodynamic radius as determined from the dynamic light scattering experiments decreases monotonically, from 214 to 90 Å, with increasing elution volume. The results from two completely independent sets of samples agree to within the experimental uncertainty as shown in Figure 1B. The individual fractions were found to be quite monodisperse, with a polydispersity index of $\simeq$20–30% at all scattering angles investigated. This is supported by the fact that the $z$-average hydrodynamic radius $\langle R_H \rangle_z$ is almost independent of $Q$, as indicated by the error bars in Figure 1B, which represent the standard deviation from the measurements at all five angles.

The molecular weights of the proteins examined ranged from a low of 440 kDa to a high of 3500 kDa. Figure 1C shows the dependence of $\langle M \rangle_w$ upon the elution volume as obtained from the static light scattering experiments. The error bars shown were deduced from a propagation of error analysis and mainly reflect the uncertainties in protein concentration and $dn/dc$. Two typical individual measurements of the angular dependence of the scattered intensity for different protein fractions are shown in Figure 2. The data are plotted as $\langle I_{ref}(Q)/I_0 \rangle / \langle \Delta I(Q)/I_0 \rangle$ vs $Q^2/3$. The linearity of the fit strongly supports the approximation for the particle

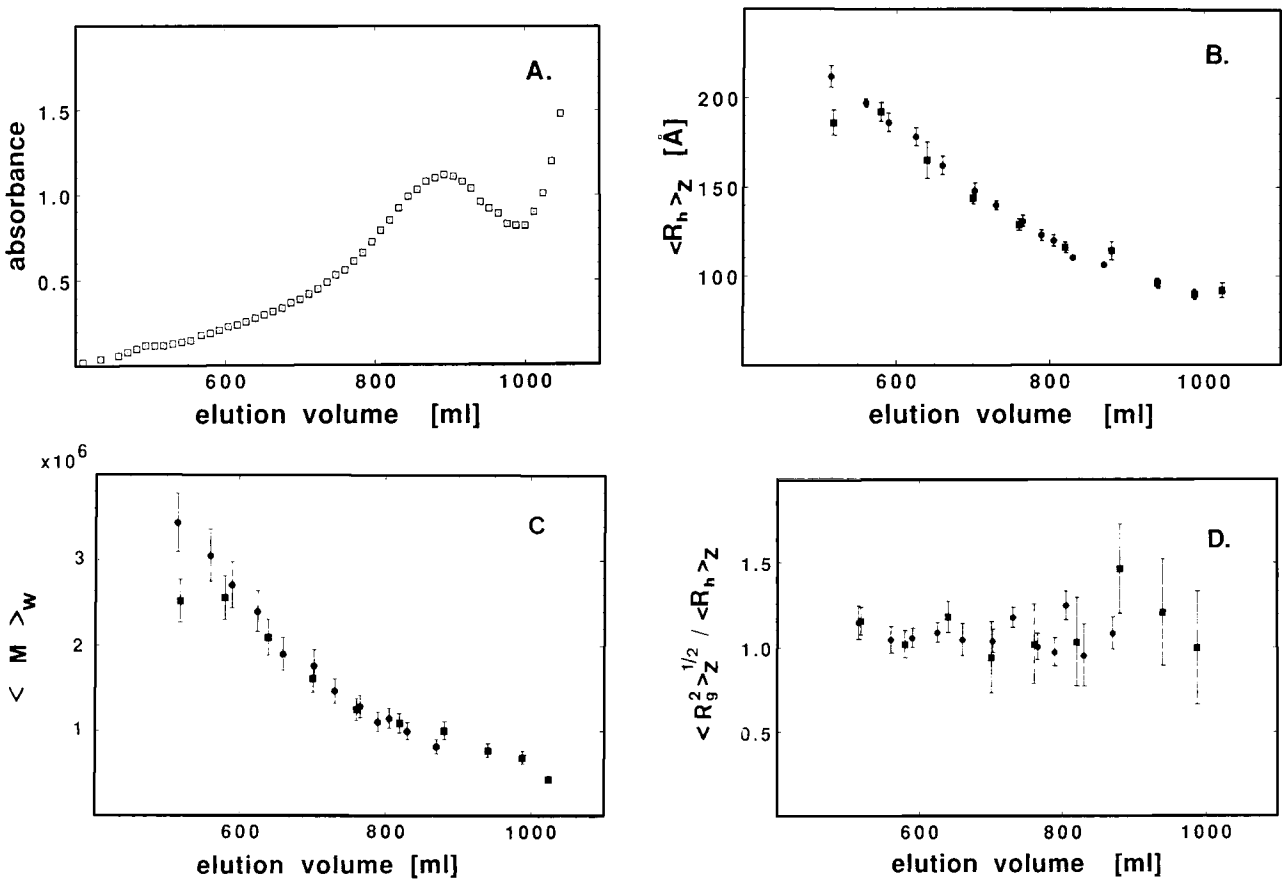


**Figure 1.** (A) Expanded elution profile of bovine nuclear lens proteins on Sepharose CL4B. (B) The $z$-average hydrodynamic radius $\langle R_H \rangle_z$ vs elution profile for individual fractions. Error bars represent standard deviation from measurements at five different scattering angles. (C) Weight average molecular weight $\langle M \rangle_w$ vs elution volume. Error bars were derived from a propagation of error analysis. (D) Ratio $\langle R_G^2 \rangle_z^{1/2} / \langle R_H \rangle_z$ vs elution volume. Error bars from propagation of error analysis. Shown are measurements from two individual preparations, A (■) and B (●).

scattering form factor $P(\theta)$ used in Eq. (2). The average radius of gyration $\langle R_G^2 \rangle_z^{1/2}$ was estimated from a weighted least-squares fit of the data to Eq. (3) as described in Materials and Methods. The results are shown in Figure 1D as a plot of the ratio $\langle R_G^2 \rangle_z^{1/2} / \langle R_H \rangle_z$ vs the elution volume. The substantially larger uncertainties in $\langle R_G^2 \rangle_z^{1/2}$ (as estimated from the statistical uncertainties of the least-squares fit parameters) compared with those for $\langle R_H \rangle_z$, in particular at large elution volumes, arise from the weak angular dependence of the scattering intensity for particles in this size range.

An analysis of the dynamic and static light scattering experiments as described in Materials and Methods is based on the assumption of ideal macromolecular solutions without interparticle interactions. Interactions between individual proteins would strongly influence both the measured diffusion coefficient as well as the apparent molecular weight.[36] We have thus investigated the dependence of $\langle R_H \rangle_z$, $\langle R_G^2 \rangle_z^{1/2}$, and $\langle M \rangle_w$ upon protein concentration. The data are summarized in Figure 3. We did not observe any measurable changes in these quantities for concentrations between 0.90 and 0.041 mg/mL, indicating the absence of detectable contributions from interparticle interaction effects.

Information on the shape of macromolecules in solution can be obtained from a quantitative comparison of the results from static (i.e., $\langle R_G^2 \rangle_z^{1/2}$ and $\langle M \rangle_w$) and dynamic (i.e., $\langle R_H \rangle_z$) light scattering experiments.[20,36,37] The results of such an analysis are summarized in Figures 1D and 4. The ratio of $\langle R_G^2 \rangle_z^{1/2} / \langle R_H \rangle_z$ varies between approximately 0.95 ± 0.15 at high elution volume or low molecular weight, and 1.10 ± 0.08 at low elution volume or high molecular weight (Figure 1D). These values

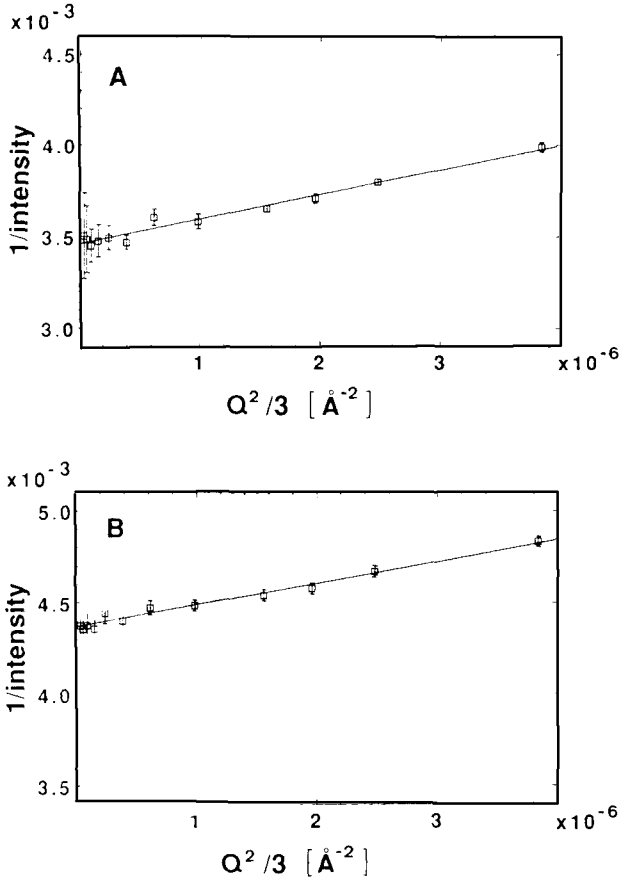


**Figure 2.** Inverse normalized scattering intensity $\langle I_{ref}(Q)/I_0\rangle/\langle I(Q)/I_0\rangle$ vs $Q^2/3$ for two different individual fractions: (A) elution volume = 590 mL, concentration = 0.37 mg/mL; (B) elution volume = 730 mL, concentration = 0.53 mg/mL. Symbols represent an average of 50 measurements and the error bars indicate the standard deviation of these measurements. Solid lines are weighted least-squares fit of Eq. (3) to the data points.

should be compared with the theoretical value of 0.78 for a spherical particle. A deduction of $\langle R_G^2\rangle_z^{1/2}$ is quite difficult for samples at the highest elution volumes studied (i.e., for elution volume >850 mL), since the angular dependence of the scattered intensity is approaching the resolution limit of our light scattering spectrometer. Based on the experimental uncertainties we cannot therefore completely rule out a spherical shape for the proteins present in these fractions. However, at low elution volume and correspondingly higher molecular weight the measured values of $\langle R_G^2\rangle_z^{1/2}$ and $\langle R_H\rangle_z$ are clearly inconsistent with a dense spherical quaternary structure of the $\alpha$-crystallin present in these fractions.

In order to obtain further information on the size and shape of $\alpha$-crystallin from nuclear extract, and to quantitatively test the consistency of the static and dynamic light scattering measurements, we have calculated $R_H$, $R_G$, and $M_w$ using theoretical models for different geometrical structures. The results for $R_G$ and $M_w$ for monodisperse spheres, short rigid cylinders, and semiflexible chains together with the experimentally determined values are shown as a function of $R_H$ in Figure 4. The molecular weight as a function of the hydrodynamic radius (Figure 4B) for the different geometries was calculated from the volume $V$ of the particle. A "density" was chosen separately for each shape so as to obtain a molecular weight of 800 kDa at a hydrodynamic radius $R_H$ = 100 Å. This normalization procedure gave the relationships $M = V/5.27$ (spheres), $M = V/4.35$ (rigid cylinders), and $M = V/5.09$ (wormlike chains). The experimental data for the higher molecular weight proteins found at low elution volume are clearly not consistent with a spherical shape. A certain amount of geometrical anisotropy is required to account for the dependence of $\langle R_G^2\rangle_z^{1/2}$ and $\langle M\rangle_w$

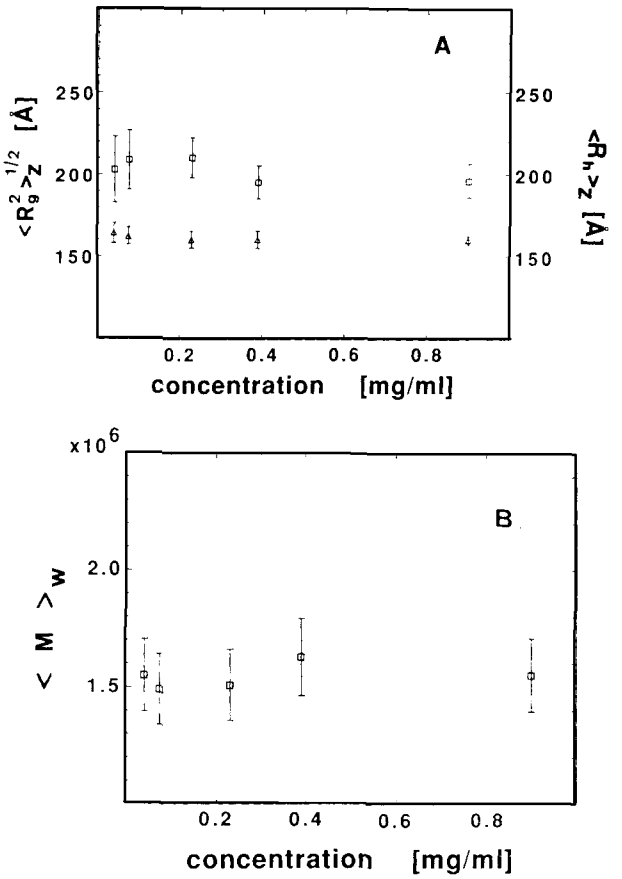


**Figure 3.** Concentration dependence of (A) $\langle R_H\rangle_z$ (△) and $\langle R_G^2\rangle_z^{1/2}$ (□), and (B) $\langle M\rangle_w$ (□), as determined by dynamic and static light scattering.

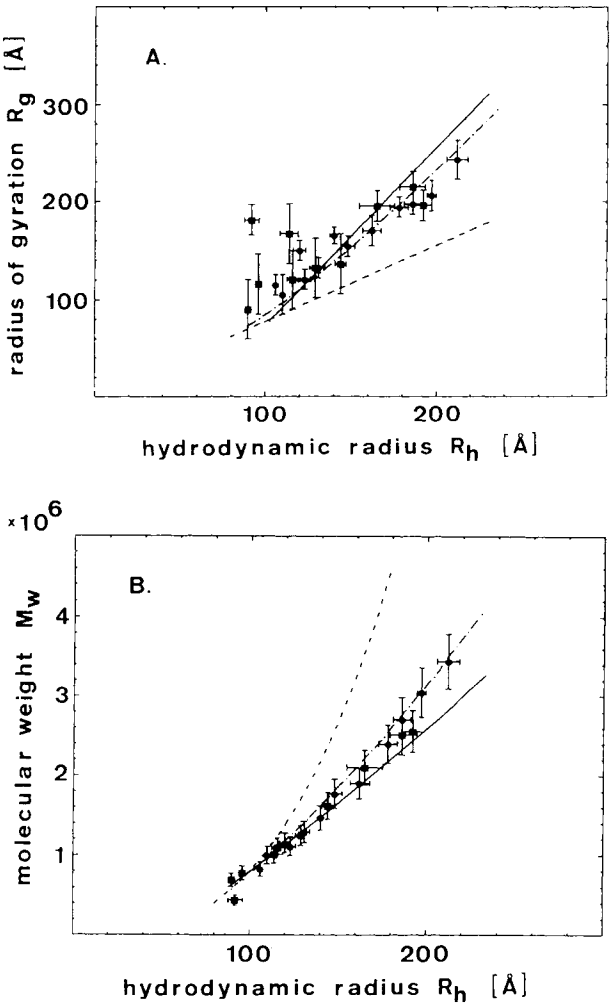


**Figure 4.** (A) Radius of gyration $\langle R_G^2 \rangle_z^{1/2}$ and (B) molecular weight $\langle M \rangle_w$ as a function of the hydrodynamic radius $\langle R_H \rangle_z$. Also shown are theoretical model calculations for sphere (- - -), rigid cylinder, $d$ = 130 Å (——), semiflexible chain, $d$ = 130 Å, $l_p$ = 400 Å (-·-·-).

on $\langle R_H \rangle_z$. Quite good agreement between theory and experimental data can be found for a model of a cylinder with a diameter of 135 Å. The agreement can be further improved by allowing a certain amount of flexibility for the cylinders (see Figure 4). This was achieved by using the model of a semiflexible ("wormlike") chain in order to describe the conformational behavior of α-crystallin aggregates in solution.[13,14] Although it was originally developed in order to understand and model the conformational behavior of synthetic polymers in solution, i.e., for macromolecules having a significantly larger length/diameter ratio, it has recently been shown that the model can be successfully applied to biopolymer systems. It does, for example, provide an excellent description of the conformational behavior of linear antigen-antibody complexes that have dimensions comparable to α-crystallin.[20]

The data shown in Figure 4 are in agreement with the results of the electron microscopy experiments performed on the same fractions.[5] These studies have indicated the presence of linear chains or rods, consisting of variable numbers of particles of circular cross section and diameters of 130–140 Å. While a detailed description of the results is given elsewhere,[5] we have listed the observed chain-length distribution (i.e., average number of particles per chain, $\langle P/C \rangle_w$) in Table I. The good agreement between the experimental data and the theoretical model calculations for semiflexible chains clearly supports the conclusions from electron microscopy.[5,6] We can thus try to quantitatively compare the light scattering results with those from electron microscopy. It is, in particular, possible to estimate $\langle M \rangle_w$, $\langle R_G^2 \rangle_z^{1/2}$, and $\langle R_H \rangle_z$ from an analysis of the chain length distribution (i.e., number of monomeric particles per chain) as obtained from electron microscopy for different fractions, and compare them with the corresponding values obtained by means of static and dynamic light scattering.

In the case of a polydisperse solution containing $N_i$ complexes built from $i$ monomeric units of molecular weight $M_1$, $\langle M \rangle_w$ can be calculated using Eq. (8):

$$\langle M \rangle_w = \frac{\sum_i N_i \cdot (i \cdot M_1)^2}{\sum_i N_i \cdot (i \cdot M_1)} = M_1 \cdot \frac{\sum_i N_i \cdot i^2}{\sum_i N_i \cdot i} \; (= M_1 \cdot \langle P/C \rangle_w) \qquad (8)$$

The results from such an analysis are summarized in Table I for different fractions obtained from two independent protein preparations. An average value of $(7.8 \pm 1.5) \cdot 10^5$ can be calculated for $M_1$, which is quite close to the values generally obtained for α-crystallins from the cortex of the lens.[1-3,6,33,35]

We can also calculate $\langle R_G^2 \rangle_z^{1/2}$ and $\langle R_H \rangle_z$ from the chain length distribution. In these calculations, the electron microscopy data[5] were employed, together with Eqs. (9) and (10)—

$$\langle R_G^2 \rangle_z^{1/2} = \left[ \frac{\sum_i N_i M_i^2 \langle R_G^2 \rangle_i}{\sum_i N_i M_i^2} \right]^{1/2} \qquad (9)$$

$$\langle R_H \rangle_z = \left[ \frac{\sum_i N_i M_i^2 (1/R_{H,i})}{\sum_i N_i M_i^2} \right]^{-1} \qquad (10)$$

in order to estimate overall values of the $z$-average radius of gyration and hydrodynamic radius for each of the fractions. For the individual chains containing $i$ monomers, $\langle R_G^2 \rangle_i$ and $R_{H,i}$ were calculated by inserting $L = i \cdot 135$, $d = 135$, and $l_p = 400$ Å into the theoretical expressions for the model of a wormlike chain.[13,14,20] The results of this analysis are also shown in Table I, and permit a further direct and quantitative comparison of the particle size distributions obtained from electron microscopy with the results of our light scattering experiments.

## DISCUSSION

The heterogeneity of $\alpha$-crystallin has stimulated the development of several structural models for the low and high molecular weight forms of the protein. In particular, it has been postulated that the formation of chain-like polymers of spherical monomeric $\alpha$-crystallin molecules can occur.[6] The independent measurements of $\langle R_G^2 \rangle_z^{1/2}$, $\langle M \rangle_w$, and $\langle R_H \rangle_z$ using light scattering and EM presented in this article are consistent with a polymerization of $\alpha$-crystallin into linear semiflexible chains consisting of monomer units with spherical cross section and with a diameter of approximately 130–140 Å. However, care has to be taken when trying to estimate the average molecular weight of these monomers, since breakdown of the polymer chain may occur during the preparation of the electron micrograph samples. This could explain the significantly different average values obtained for $M_1$ of $(6.7 \pm 0.6) \cdot 10^5$ and $(8.7 \pm 1.4) \cdot 10^5$, respectively, for the two different preparations, since the results from the light scattering experiments agree within the experimental uncertainties for the two preparations (see also Figure 1).

The possibility of partial chain breakdown during the preparation of the electron microscopy samples is further supported by the results of the calculation of $\langle R_G^2 \rangle_z^{1/2}$ and $\langle R_H \rangle_z$ from the chain length distribution (Table I). Despite the large uncertainty of these model calculations of the conformational and hydrodynamic properties of protein solutions, the deduced values of $\langle R_G^2 \rangle_z^{1/2}$ and $\langle R_H \rangle_z$ are significantly lower than those determined from light scattering, which would also be consistent with a partial chain breakdown during the sample preparation for the electron microscopy. The molecular weight $M_1$ could thus be significantly lower than the obtained average value of 780 kDa. Populations of $\alpha$-crystallins with a molecular weight of approximately 400–500 kDa and diameters of 130–140 Å can in fact be

**Table I Observed and Calculated Hydrodynamic Parameters for Bovine $\alpha$-Crystallins**

| Elution Volume (mL) | Particles/ Chain ($\langle P/C \rangle_w$) | Molecular Weight (kDa) | | $R_G$ (Å) | | $R_H$ (Å) | |
|---|---|---|---|---|---|---|---|
| | | $\langle M \rangle_w$ | $M_1$[a] | Observed | Calculated[b] | Observed | Calculated[b] |
| | | | | Preparation A | | | |
| 518 | 4.37 | 2520 | 580 | 215 ± 15 | 212 | 186 ± 7 | 167 |
| 580 | 3.46 | 2560 | 740 | 196 ± 15 | 169 | 192 ± 5 | 145 |
| 640 | 3.04 | 2100 | 690 | 195 ± 15 | 149 | 165 ± 10 | 136 |
| 700 | 2.4 | 1620 | 680 | 136 ± 30 | 123 | 144 ± 3 | 120 |
| 880 | 1.51 | 1010 | 670 | 120 ± 30 | 92 | 114 ± 5 | 101 |
| | | | | Preparation B | | | |
| 508 | 3.91 | 3710 | 950 | 243 ± 20 | 179 | 212 ± 6 | 153 |
| 553 | 3.37 | 3120 | 930 | 206 ± 15 | 161 | 194 ± 2 | 142 |
| 584 | 2.90 | 2760 | 950 | 200 ± 10 | 142 | 185 ± 5 | 131 |
| 653 | 2.19 | 2080 | 950 | 180 ± 10 | 111 | 170 ± 5 | 115 |
| 701 | 1.91 | 1660 | 870 | 150 ± 10 | 101 | 145 ± 5 | 108 |
| 781 | 1.68 | 1280 | 760 | 135 ± 10 | 92 | 125 ± 5 | 103 |
| 880 | 1.51 | 910 | 600 | 110 ± 15 | 96 | 105 ± 5 | 103 |

[a] $M_1$, the molecular weight of a single 135 Å particle, was calculated using the chain-length distribution as determined from electron microscopy[5] and Eq. (8) presented in the text.

[b] $R_G$ and $R_H$ for a semiflexible chain of 135 Å diameter and 400 Å persistence length were calculated using Eqs. (9) and (10), respectively, together with the chain-length distribution from electron microscopy.[5]

isolated by repeated fractionation[35] or by reaggregation of denatured protein at low temperatures.[10]

Our data thus suggest that the age-related increase in the size of $\alpha$-crystallin aggregates can be attributed to the polymerization of monomeric species. This would be consistent with the observed increase in chainlike polymers in the aging lens.[6]

It is interesting to compare our light scattering results from fractions at high elution volume containing mainly monomeric units, which yielded $\langle R_H \rangle_z \simeq 95 \pm 3$ Å and $\langle R_G^2 \rangle_z^{1/2} / \langle R_H \rangle_z \simeq 0.95$, with the results of a recent study reporting small angle x-ray (SAXS) and dynamic light scattering experiments on $\alpha$-crystallins from cortical extracts.[33] These authors found a value of $R_H = 88 \pm 2$ Å for the hydrodynamic radius. From a Guinier plot of the SAXS data they deduced a value of $R_G = 61 \pm 1$ Å for the radius of gyration. Based on these results they developed a complex, three-layered spherical model for the quaternary structure of $\alpha$-crystallin. This model is similar to that of Siezen et al.,[1] and proposes that only the inner two layers are filled with subunits in the young (cortical) protein and that the age-related size increase is due to the addition of subunits in the outer layer.

The data of Tardieu et al.,[33] and the conclusions arising from them, are different from those of the present study. Most likely, the differences may be attributed to differences in the protein preparation and handling. Tardieu et al. studied unfractionated populations of cortical $\alpha$-crystallins. These were heterogeneous and appeared to be unstable since their hydrodynamic properties were found to change with time after the isolation. Their molecular weights were found to decrease from as high as 1100 ± 100 kDa to 840 ± 80 kDa, and corresponding changes in $R_G$ and $R_H$ were noted. By contrast, highly fractionated nuclear $\alpha$-crystallins were examined in the present study, and no time-dependent changes were observed in their hydrodynamic properties over a prolonged period of time. In addition, different buffer conditions were used that may have a significant influence on the quaternary structure of $\alpha$-crystallin.[33]

However, one should not only focus on the preparation conditions, but also keep in mind the different experimental approaches and their corresponding limitations used in these studies. A commonly used analysis method in SAXS is the determination of the radius of gyration $R_G$ through the law of Guinier, which is based on an expansion of the scattering intensity at small $Q$ values [Eq. (2)].[38] This expansion is only valid for $R_G \cdot Q \ll 1$ if no a priori knowledge on the shape of the particles is available. If the shape of the scattering particles is known, other expansions can be used, which remain valid up to $R_G \cdot Q \simeq 1$ (for larger $Q$ values, a nonlinear $Q^2$ dependence can be expected even for monodisperse particles due to the higher order minima and maxima of the particle form factor).[39] For globular particles, Guinier's expression

$$\ln \frac{I(Q)}{I(0)} \simeq -\frac{Q^2 R_G^2}{3} \tag{11}$$

can be applied, and $R_G$ can be obtained from a Guinier plot of $\ln[I(Q)]$ vs $Q^2$. For polydisperse particles, additional difficulties and possible sources for artefacts in the data analysis procedure arise. For polydisperse spheres, the average intensity in the absence of interparticle interaction effects can be computed according to

$$I(Q) = N_p \langle |F(Q)|^2 \rangle = N_p \int_0^\infty |F(Q, R)|^2 f(R) dR \tag{12}$$

where $N_p$ is the number density of particles, $F(Q, R)$ is the (intraparticle) scattering form factor of a sphere of radius $R$, and $f(R)$ is the distribution function describing the size distribution of the particles. Even moderate polydispersity tends to smear out the otherwise well-defined intensity minima and maxima at high $Q$ values, and the scattering from polydisperse spheres is, for example, often indistinguishable from the scattering from ellipsoids, in particular, from prolate ellipsoids.[39,40] A Guinier representation can also lead to wrong results when an interference peak [or a steep rise in $S(Q)$] due to strong interparticle interaction effects has not been recognized at low $Q$ values, because it is located below the lowest $Q$ value accessible to the instrument. In this case, the measured $R_G$ will be strongly influenced or even completely determined by the tail of such interparticle interferences.[39] As a practical consequence, for compact particles the largest dimensions should be determined not only from a Guinier approximation, but also with much higher accuracy from the oscillations of the scattering intensity at high $Q$. It is interesting to note in this regard that Tardieu et al. did in fact deduce $R_G$ from Guinier plots in a range corresponding to $1 < Q \cdot R_G < 2$. This range of scattering vectors was chosen because a downward curvature of $\ln I(Q)$ vs $Q^2$ was sometimes visible at low $Q$, indicating a measurable

influence of interparticle interaction effects on the scattering intensity.[33]

As a consequence, we have first reduced the heterogeneity of the $\alpha$-crystallins by means of gel filtration. The stability of the samples was carefully monitored in order to ensure that no time-dependent changes in the hydrodynamic properties of the proteins occurred after fractionation. A special effort was made in order to combine the results from different and complementary experimental techniques. Scattering experiments were performed at different protein concentrations, and no indication of any contributions from interparticle interaction effects could be observed at the low protein concentrations used in this study. Even though our results obtained with high elution volume fractions still indicate some anisotropy of the protein, we cannot rule out completely a spherical structure for these low molecular weight proteins due to the resolution limit of our spectrometer at $R_G \leq 80$ Å. This is a limitation of the light scattering experiment as compared to SAXS or small angle neutron scattering (SANS). Therefore it would be desirable to also perform SAXS or SANS on the same samples, thus extending the characteristic probing distance $(1/Q)$ of the scattering experiment to much lower values. However, the results obtained at low elution volume are clearly inconsistent with a spherical growth of the protein and support the presence of linear aggregates in these solutions.

It is also interesting to compare our results with a detailed light scattering and fluorescence study of cortical $\alpha$-crystallin.[41,42] These authors looked at the concentration dependence of the collective and tracer diffusion coefficient at moderate concentrations, i.e., volume fractions $0.005 \leq \Phi \leq 0.025$. Under these conditions, the results could be interpreted in terms of simple two-body interaction potentials between spherical particles. At high concentrations, i.e, $0.035 \leq \Phi \leq 0.125$, QLS experiments indicated a reversible formation of clusters, giving rise to a second and slowly decaying component in the intensity correlation function. Our study represents an extension of this work to much lower concentrations ($3 \cdot 10^{-5} \leq \Phi \leq 8 \cdot 10^{-4}$) and fractionated nuclear $\alpha$-crystallins. Under these conditions, no concentration dependence of $\langle R_H \rangle_z$, $\langle R_G^2 \rangle_z^{1/2}$, and $\langle M \rangle_w$ could be observed due to a negligible influence of interparticle interaction effects. However, it would be most interesting to study the concentration dependence of the different fractions. This would allow us to profit from the enormous theoretical progress on the interaction dependence of static and dynamic properties such as the osmotic compressibility, $\langle R_H \rangle_z$, or $\langle R_G^2 \rangle_z^{1/2}$ for colloid[43-45] and polymer solutions.[12,46,47] In particular, the applicability of hard-sphere models to high elution volume fractions, where monomeric proteins are expected to dominate, and the recently found universality for static and dynamic correlation lengths[46,47] (which correspond to $R_G/3^{1/2}$ and $R_H$ for dilute solutions, respectively) of synthetic polymers to low elution volume fractions, where polymerlike aggregates can be found, could be tested.

## CONCLUSIONS

We have measured $\langle R_H \rangle_z$, $\langle R_G^2 \rangle_z^{1/2}$, and $\langle M \rangle_w$ for individual fractions of bovine $\alpha$-crystallin from nuclear extracts. A strong and monotonic decrease of $\langle R_H \rangle_z$ and $\langle M \rangle_w$ with increasing elution volume could be observed, indicating a quite broad size distribution. Whereas the size of the proteins at high elution volume is too small in order to unambiguously determine their shape, the data at low elution volume clearly indicates the formation of anisotropic high molecular weight aggregates. The experimental results are quantitatively consistent with a polymerization of monomeric units into linear chains, which may have a certain degree of flexibility.

Using theoretical expressions for $\langle R_G^2 \rangle$ and $R_H$ originally derived for semiflexible polymers in solution, we can self-consistently analyze the data from electron microscopy and static and dynamic light scattering experiments. We thus obtain detailed information on the molecular weight distribution and the quaternary structure of $\alpha$-crystallin in solution. The above-presented results may not answer all the open questions concerning the structure of and interactions between $\alpha$-crystallins in solution due to the specific solution conditions chosen in this study. However, even though we are still far away from a complete understanding of the complex structural properties of $\alpha$-crystallin, we now have a theoretical and experimental framework in order to overcome some of the difficulties imposed by the inherent molecular heterogeneity, which can also be extended to other biopolymer systems.

We gratefully acknowledge Professor George Benedek who kindly provided access to the light scattering apparatus located in his laboratory in the Department of Physics at MIT. This instrument was constructed using funds from NSF grant no. PCM 8313025. This work was performed while RCA was on sabbatical leave at MIT. The generosity

of Professor Benedek and the Jessie B. Cox Trust made this visit possible.

## REFERENCES


1. Siezen, R. J., Bindels, J. G. & Hoenders, H. J. (1980) *Eur. J. Biochem.* **111,** 435–444.
2. Thomson, J. A. & Augusteyn, R. C. (1983) *Exp. Eye Res.* **37,** 367–377.
3. Spector, A., Li, L.-K., Augusteyn, R. C., Schneider, A. & Freund, T. (1971) *Biochem. J.* **124,** 337–343.
4. van Kleef, F. S. M., de Jong, W. W. & Hoenders, H. J. (1975) *Nature* (London) **258,** 264–266.
5. Koretz, J. F. & Augusteyn, R. C. (1991) manuscript in preparation.
6. Siezen, R. J., Bindels, J. G. & Hoenders, H. J. (1979) *Exp. Eye Res.* **28,** 551–567.
7. Augusteyn, R. C. & Koretz, J. F. (1987) *FEBS Lett.* **222,** 1–5.
8. Thomson, J. A. & Augusteyn, R. C. (1984) *J. Biol. Chem.* **259,** 4339–4345.
9. Thomson, J. A. & Augusteyn, R. C. (1988) *Biochim. Biophys. Acta* **994,** 246–252.
10. Clauwaert, J., Ellerton, H. D., Koretz, J. F., Thomson, K. & Augusteyn, R. C. (1989) *Curr. Eye Res.* **8,** 397–403.
11. Augusteyn, R. C., Koretz, J. F. & Schurtenberger, P. (1989) *Biochim. Biophys. Acta* **999,** 293–299.
12. Schaefer, D. W. & Han, C. C. (1985) in *Dynamic Light Scattering,* Pecora, R., Ed., Plenum Press, New York, pp. 181–243.
13. Yamakawa, H. (1971) *Modern Theory of Polymer Solutions,* Harper & Row, New York.
14. Yamakawa, H. & Fujii, M. (1973) *Macromolecules* **6,** 407–415.
15. Schmitd, M. (1984) *Macromolecules* **17,** 553–560.
16. Pecora, R., ed. (1985) *Dynamic Light Scattering,* Plenum Press, New York.
17. Candau, S. J. (1988) in *Surfactant Science Series,* Vol. 22, Zana, R., Ed., Dekker, New York, pp. 147–207.
18. Schurtenberger, P. & Hauser, H. (1984) *Biochim. Biophys. Acta* **778,** 470–480.
19. Schurtenberger, P., Svärd, M., Wehrli, E. & Lindman, P. (1986) *Biochim. Biophys. Acta* **882,** 465–468.
20. Murphy, R. M., Slayter, H., Schurtenberger, P., Chamberlin, R. A., Colton, C. K. & Yarmush, M. L. (1988) *Biophys. J.* **54,** 45–56.
21. van Holde, K. E. (1985) *Physical Biochemistry,* 2nd ed., Prentice-Hall, Englewood Cliffs, NJ.
22. Berne, B. J. & Pecora, R. (1976) *Dynamic Light Scattering.* John Wiley & Sons, New York.
23. Koppel, D. E. (1972) *J. Chem. Phys.* **57,** 4814–4820.
24. Young, C. Y., Missel, P. J., Mazer, N. A., Benedek, G. B. & Carey, M. C. (1978) *J. Phys. Chem.* **82,** 1375–1378.
25. Mazer, N. A., Benedek, G. B. & Carey, M. C. (1980) *Biochemistry* **19,** 601–615.
26. Burchard, W. (1983) *Adv. Polym. Sci.* **48,** 1–124.
27. Koretz, J. F. (1982) *Methods Enzymol.* **85**(B), 20–55.
28. Haller, H. R., Destor, C. & Cannell, D. S. (1983) *Rev. Sci. Instrum.* **54,** 973–983.
29. Coumou, D. J. (1960) *J. Colloid Sci.* **15,** 408–417.
30. Bender, T. M., Lewis, R. J. & Pecora, R. (1986) *Macromolecules* **19,** 244–245.
31. Pierscionek, B., Smith, G. & Augusteyn, R. C. (1987) *Vision Res.* **27,** 1539–1541.
32. Missel, P. J., Mazer, N. A., Benedek, G. B., Young, C. Y. & Carey, M. C. (1980) *J. Phys. Chem.* **84,** 1044–1057.
33. Tardieu, A., Laporte, D., Licinio, P., Krop, B. & Delaye, M. (1986) *J. Mol. Biol.* **192,** 711–724.
34. Augusteyn, R. C., Hum, T. P., Putilin, T. & Thomson, J. A. (1987) *Biochim. Biophys. Acta* **915,** 132–139.
35. Thomson, J. A. & Augusteyn, R. C. (1988) *Curr. Eye Res.* **7,** 563–569.
36. Schurtenberger, P., Mazer, N. & Känzig, W. (1983) *J. Phys. Chem.* **87,** 308–315.
37. van de Sande, W. & Persoons, A. (1985) *J. Phys. Chem.* **89,** 404–406.
38. Guinier, A. & Fournet, G. (1955) *Small Angle Scattering of X-Rays,* Wiley–Interscience, New York.
39. Cabane, B. (1988) in *Surfactant Science Series,* Vol. 22, R. Zana, Ed., Marcel Decker, New York and Basel.
40. Hayter, J. B. (1985) in *Physics of Amphiphiles: Micelles, Vesicles and Microemulsions,* Degiorgio, V. & Corti, M., Eds., North-Holland, Amsterdam, pp. 59–93.
41. Andries, C., Guedens, W., Clauwaert, J. & Geerts, H. (1983) *Biophys. J.* **43,** 345–354.
42. Andries, C. & Clauwaert, J. (1985) *Biophys. J.* **47,** 591–605.
43. Pusey, P. N. & Tough, R. J. (1985) in *Dynamic Light Scattering,* Pecora, R., Ed., Plenum Press, New York, pp. 85–180.
44. Vrij, A., Nieuwenhuis, E. A., Fijnaut, H. M. & Agterof, W. G. M. (1978) *Faraday Discuss. Chem. Soc.* **65,** 101–113.
45. Cannell, D. S. (1985) in *Physics of Amphiphiles: Micelles, Vesicles and Microemulsions,* Degiorgio, V. & Corti, M., Eds., North-Holland, Amsterdam, pp. 202–211.
46. Wiltzius, P., Haller, H. R., Cannell, D. S. and Schaefer, D. W. (1983) *Phys. Rev. Lett.* **51,** 1183–1186.
47. Wiltzius, P., Haller, H. R., Cannell, D. S. and Schaefer, D. W. (1984) *Phys. Rev. Lett.* **53,** 834–837.


*Received February 21, 1991*
*Accepted June 4, 1991*